THE JOURNAL OF PHYSICAL CHEMISTRY B

Article

pubs.acs.org/JPCB

Dynamics of Ground and Excited State Vibrational Relaxation and Energy Transfer in Transition Metal Carbonyls

Milan Delor,[†] Igor V. Sazanovich,[‡] Michael Towrie,[‡] Steven J. Spall,[†] Theo Keane,[†] Alexander J. Blake,[§] Claire Wilson,[§] Anthony J. H. M. Meijer,*[,†] and Julia A. Weinstein*[,†]

[†]Department of Chemistry, University of Sheffield, Sheffield S3 7HF, U.K.

[‡]Central Laser Facility, Research Complex at Harwell, Rutherford Appleton Laboratory, Harwell Science and Innovation Campus, STFC, Chilton, Oxfordshire, OX11 0QX, U.K.

[§]School of Chemistry, University of Nottingham, Nottingham NG7 2RD, U.K.

Supporting Information

ABSTRACT: Nonlinear vibrational spectroscopy provides insights into the dynamics of vibrational energy transfer in and between molecules, a crucial phenomenon in condensed phase physics, chemistry, and biology. Here we use frequency-domain 2-dimensional infrared (2DIR) spectroscopy to investigate the vibrational relaxation (VR) and vibrational energy transfer (VET) rates in different solvents in both the electronic ground and excited states of Re(Cl)$(CO)_3$(4,4′-diethylester-2,2′-bipyridine), a prototypical transition metal carbonyl complex. The strong C≡O and ester C═O stretch infrared reporters, located on opposite sides of the molecule, were monitored in the 1600−2100 cm^{-1} spectral region. VR in the lowest charge transfer triplet excited state (^{3}CT) is found to be up to eight times faster than in the ground state. In the ground state, intramolecular anharmonic coupling may be solvent-assisted through solvent-induced frequency and charge fluctuations, and as such VR rates are solvent-dependent. In contrast, VR rates in the solvated ^{3}CT state are surprisingly solvent-insensitive, which suggests that predominantly intramolecular effects are responsible for the rapid vibrational deactivation. The increased VR rates in the excited state are discussed in terms of intramolecular electrostatic interactions helping overcome structural and thermodynamic barriers for this process in the vicinity of the central heavy atom, a feature which may be of significance to nonequilibrium photoinduced processes observed in transition metal complexes in general.

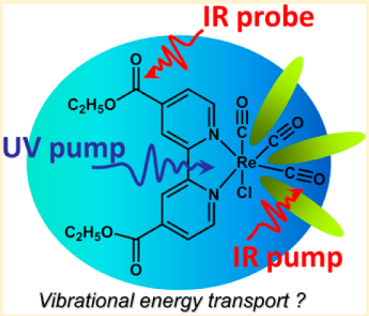

INTRODUCTION

Vibrational relaxation (VR) and energy transfer (VET) are ubiquitous and of central importance to photoinduced processes in the condensed phase.[1−3] Vibrational dynamics occurs over a wide range of time scales, ranging from femtoseconds to hundreds of picoseconds,[2] influencing the rates and mechanisms of a vast number of chemical reactions.[3] Time-resolved two-dimensional infrared (2DIR) spectroscopy allows the direct measurement of population and relaxation dynamics of vibrational modes in molecules, providing insight on relaxation pathways, energy flow, and coupling mechanisms over significant distances.[3−8]

Transition metal complexes often exhibit nonequilibrium photoinduced processes such as ultrafast intersystem crossing (ISC) and electron transfer from nonthermalized excited states.[9−15] It is known that both intra- and intermolecular structural reorganization play crucial roles in defining the rates and pathways of excited state reactions. For example, optically driven vibrational modes can explore the crossing point of spin-crossover potential surfaces and drive ISC reactions along a specific coordinate,[9−11,13] while solvent−solute interactions influence the shape of the potential energy landscape.[16,17] Similarly, electron−hole recombination in charge transfer reactions can be facilitated through high frequency vibrational modes coupling to the electronic excited state potential surfaces.[16,18] Investigating VR, intramolecular vibrational redistribution (IVR), VET and associated coupling mechanisms in transition metal systems in both ground and excited electronic states may provide insights into the complex factors controlling their excited state dynamics and how to manipulate them.

Here we use a narrowband infrared pump−broadband infrared probe 2DIR arrangement[3,5,19,20] to initiate and follow VR and VET in the electronic ground and excited states of a prototypical transition metal complex. The excited state is accessed by introducing a UV pump before the IR pump−probe pulse sequence (Figure 1A).[21] This pulse sequence allows unambiguous isolation of vibrational relaxation and energy transfer from electronic relaxation and solvation dynamics because the long (>nanosecond) lifetime of the excited state under investigation allows these processes to fully relax before introducing the IR pump−probe sequence. This

Received: June 25, 2014
Revised: August 26, 2014
Published: September 8, 2014

dx.doi.org/10.1021/jp506326u | J. Phys. Chem. B 2014, 118, 11781−11791

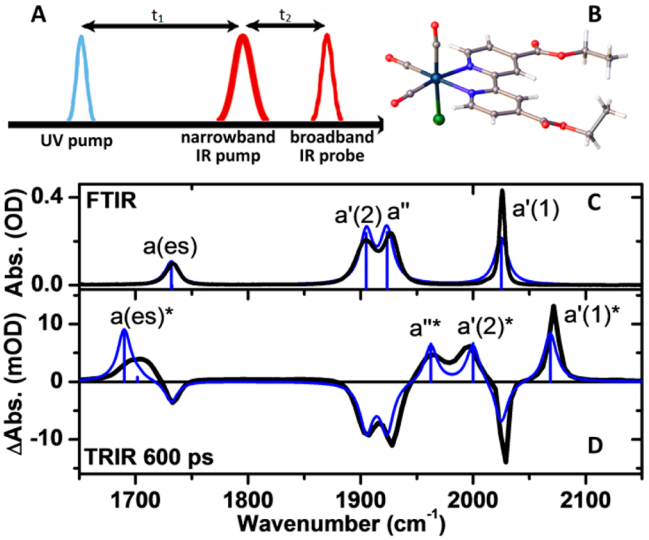

Figure 1. (A) Pulse sequence used in the excited state 2DIR experiments; t_1 is kept at 600 ps. The ground state 2DIR experiments are performed without the UV pump. (B) X-ray structure of ReCOe; the structure of the DFT-optimized singlet state matches the X-ray structure satisfactorily (the overlap is shown in Supporting Information, Figure S6). (C) Ground state Fourier transform infrared (FTIR) spectrum of ReCOe in CD_2Cl_2. (D) Time-resolved IR (TRIR) spectrum 600 ps after 400 nm excitation. Asterisks denote excited state bands. Blue lines are calculated spectra with an anharmonic scaling factor of 0.9763, a fwhm of 7 cm^{-1}, and with intensities scaled to the ground state a(es) band. The calculated TRIR spectrum is obtained by subtracting the ground singlet state IR spectrum from the lowest triplet state IR spectrum. See text for details of assignments.

task cannot be achieved using one-dimensional time-resolved infrared spectroscopy.

The model system chosen to be analyzed in this study is $Re(Cl)(CO)_3$(4,4′-diethylester-2,2′-bipyridine), ReCOe (Figure 1B). Carbonyl complexes of Re^I with diimine ligands have been extensively investigated because of their exceptionally rich photophysics[11,17,22] leading to applications as photosensitizers,[23,24] photocatalysts for CO_2 reduction,[25,26] and triggers for electron transfer reactions[27] stemming from the charge-transfer nature of their excited states. Their high-frequency C≡O stretching vibrations are excellent infrared reporters, and as such they have served as model systems for 2DIR spectroscopy.[21,26,28−31] Recently, 2DIR has been used to study VR and VET in the electronic ground state of several other metallocarbonyl complexes,[28,32,33] while excited state 2DIR was applied to study solvation dynamics,[34] as well as solute reorientational and vibrational dynamics of hot photoproducts formed by UV photolysis.[35−40] To the best of our knowledge, direct measurements and comparison of ground and solvated excited state vibrational dynamics have yet to be undertaken.

In ReCOe, a C═O group of the ester functionality on the bipyridine unit serves as an infrared reporter on the opposite side of the molecule to the C≡O groups. C═O and C≡O stretching frequencies are separated in space by approximately 8−9 Å, but are separated in energy by some 300 cm^{-1}, thus giving an opportunity to probe long-range VET across the molecule with a single broadband pulse. The direct comparison of vibrational dynamics in the ground and excited states of ReCOe in different solvents (CD_2Cl_2, CH_2Cl_2, toluene, MeCN) allows us to investigate the effects of both intra- and intermolecular interactions, as well as how charge distribution affects vibrational coupling in this model transition metal carbonyl complex.

EXPERIMENTAL DETAILS

The TRIR and 2DIR two/three-pulse experiments were performed on the ULTRA system at the STFC Central Laser Facility, Rutherford Appleton Laboratories, described elsewhere in detail.[41,42] Three-pulse experiments use optical choppers modulating the repetition rate of the UV pump at 5 kHz and IR pump at 2.5 kHz while the probe pulse is at 10 kHz, facilitating the simultaneous collection of background, UV pump−IR probe (TRIR), IR pump−IR probe (ground state 2-dimensional IR) and UV pump−IR pump−IR probe (excited state 2-dimensional IR or IR previbrationally excited TRIR depending on the order of the two pumps) data.

The tunable IR pump (∼12 cm^{-1} bandwidth) and probe (400 cm^{-1} bandwidth) pulses used for double-resonance 2D-IR spectroscopy were generated by two optical parametric amplifiers pumped by synchronized Ti:sapphire-based regenerative amplifiers with ps and fs pulse duration, respectively. The 400 nm pump beam was generated from the second harmonic of the fs laser. The probe spectrum was recorded via a HgCdTe array detector and spectrometer combination that yielded a spectral resolution of 2 cm^{-1}.

For the data shown in the text, beam energies were approximately 0.5 μJ/pulse for both UV and IR pumps, with spot sizes of approximately 80, 100, and 150 μm for IR probe, IR pump, and UV pump, respectively. The pump−probe polarization relationships were set to magic angle to remove the effects of molecular rotation in all 2-pulse experiments. In 3-pulse experiments, UV and IR pumps were set parallel to each other and the probe beam was set at magic angle with respect to these pumps. Samples were flowed and rastered in Harrick cells. UV−vis absorption and FTIR spectra were taken before and after every experiment to check for any decomposition. Optical densities at the excitation wavelength (400 nm) were kept at approximately 0.5.

Synthesis of ReCOe. $Re^I(CO)_5Cl$ (290 mg, 0.80 mmol) and 4,4′-diethylester-2,2′-bipyridine (245 mg, 0.82 mmol) were put in a Schlenk tube, and placed under Ar atmosphere by three vacuum−Ar cycles; 60 cm^3 of dry Ar-saturated toluene was added, and the mixture was left to reflux for 15 h resulting in an orange reaction solution. The solution was then dried using a rotary evaporator, and the product obtained was purified using a silica packed column with 99:1 DCM/methanol mobile phase. The amount obtained was 293 mg (0.51 mmol, 64% yield). ^{1}H NMR (250 MHz, $CDCl_3$, ppm) δ = 9.23 (dd, 5.7 Hz, 0.6 Hz; 2H), 8.85 (d, 0.9 Hz, 2H), 8.11 (dd, 5.7 Hz, 1.6 Hz; 2H), 4.57 (q, 7.1 Hz; 2H; CH_2), 1.51 (t, 7.1 Hz; 3H, CH_3). The UV−vis spectrum is shown in Supporting Information, Figure S4. Single crystals suitable for X-ray diffraction were grown by slow diffusion of Et_2O into a solution of the complex in THF at room temperature (rt), and an orange block crystal, 0.32 × 0.16 × 0.15 mm^3 was analyzed. The details of X-ray structure determination are given in the Supporting Information (Tables S2−S6, Figure S5), and a ball-and-stick representation of the structure is shown in Figure 1B.

Density Functional Theory (DFT). All calculations were performed using Gaussian 09, version C.01,[43] compiled using Portland compiler v 8.0-2 with the Gaussian-supplied versions of ATLAS and BLAS,[44] using the B3LYP functional of DFT.[45]

dx.doi.org/10.1021/jp506326u | J. Phys. Chem. B 2014, 118, 11781−11791

In all cases an extensive basis set was used, consisting of 6-311G(d,p)[46] on all elements apart from rhenium, which was described using a Stuttgart−Dresden pseudopotential.[47] In previous work it was found that this results in a reasonably accurate description of transition-metal complexes and their properties,[48,49] allowing for semiquantitative comparison with experiment. In all calculations the bulk solvent was described using PCM,[50] whereby the standard parameters for dichloromethane as supplied in Gaussian were used. An ultrafine integral grid was used. All structures were confirmed to be minima through the absence of imaginary frequencies, which were calculated in the harmonic approximation.

RESULTS

The Fourier transform infrared (FTIR) spectrum in Figure 1C shows the ground state IR absorbance of ReCOe in CD_2Cl_2. The annotated assignments are based on published material,[31] as well as DFT calculations which agree with previous assignments and reproduce the IR spectrum well. The bands at 2025, 1927, 1904, and 1733 cm^{-1} are assigned to a′(1) (symmetric stretching of all C≡O groups), a″ (antisymmetric stretching of equatorial C≡Os), a′(2) (antisymmetric stretching of axial vs equatorial C≡Os) and a(es) (two almost overlapping transitions corresponding to symmetric and antisymmetric stretching of ester C═Os, with the antisymmetric contribution dominating), respectively.

Figure 1D shows the time-resolved IR (TRIR) spectrum 600 ps after 400 nm excitation of ReCOe in CD_2Cl_2, that is, once the solute is vibrationally relaxed and fully solvated. The excited state evolution of very similar complexes of the type Re(diimine)$(CO)_3$X is well documented.[11,17,22,51−54] The spectrum at 600 ps corresponds to the lowest triplet, a charge transfer (^{3}CT) state of predominantly Re/Cl → bpy character. This is consistent with the observed positive shift of the ν(C≡O) bands and negative shift of ν(C═O) in this excited state, originating from a shift of electron density away from the metal center toward the 4,4′-diethylester-2,2′-bipyridine unit which reduces π back-donation to the antibonding π^* orbital of the −C≡O ligands and increases population of the antibonding orbital of the −C═O ligands.[51,54−56] Calculated infrared frequencies for the lowest triplet state within the harmonic approximation are in good agreement with experiment. The assignments are annotated in Figure 1D. Anharmonic calculations show that there are several combination bands in the area of interest in the lowest triplet state, in particular those at 2030 and 2054 cm^{-1} corresponding to [backbone torsional + a′(2)*] and [backbone torsional + a″*] modes. These combination bands are detailed in the Supporting Information.

Vibrational mode frequencies and line widths are highly sensitive to their environments.[4] Consequently, the position of the intense and well-defined high frequency C≡O modes in metal carbonyls have been extensively used as probes of electrostatic and solvation microenvironments.[22,28,51−53,57−59,] The larger line widths in the CT state can be, among other factors, an indication of increased frequency fluctuations and of reduction in symmetry.[56,57,60]

Figure 2 shows ground state 2-dimensional IR (GS2DIR) maps of ReCOe in CD_2Cl_2 at 1 and 10 ps delays (A,B), and 1-D pump−probe slices (several delay times at a single pump frequency) upon excitation of the a′(1) band at 2025 cm^{-1} (C,D) and of the a(es) band at 1730 cm^{-1} (E). When the IR pump is resonant with the 0 → 1 transition of a particular vibration, the ν = 0 mode of that vibration is partially depleted

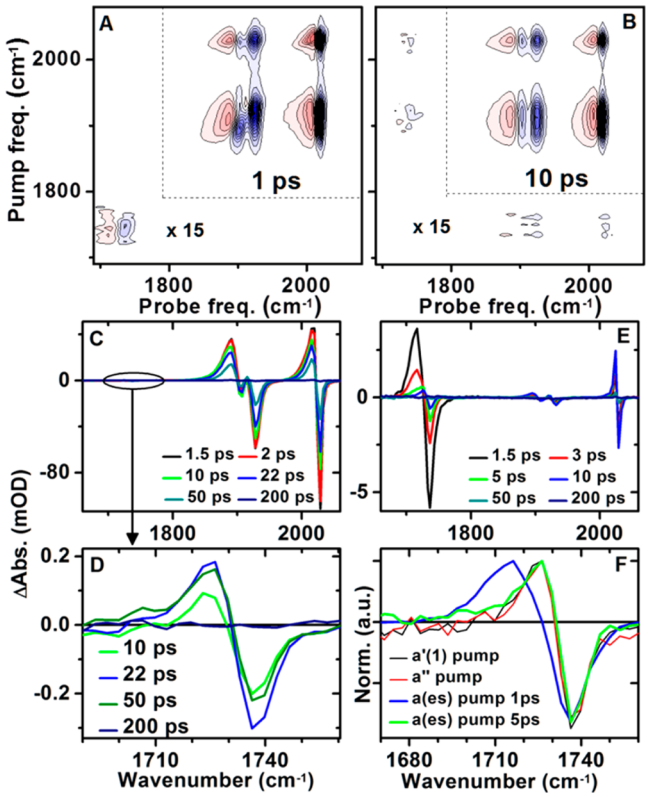

Figure 2. Ground state 2DIR spectra of ReCOe in CD_2Cl_2. (A, B) 2D maps at 1 and 10 ps IR pump−IR probe delay, respectively. Colors correspond to −25 mOD (blue) and +25 mOD (red). (C) Pump−probe 1D spectrum at representative delay times after exciting a′(1) (ca. 2025 cm^{-1}). (D) Close-up of the a(es) probe region at early time delays following a′(1) excitation. (E) Pump−probe 1D spectrum at representative delay times after exciting a(es) (ca. 1730 cm^{-1}). (F) Normalized spectra of the a(es) response (probe) to the excitation (pump) of several different vibrations. The a(es) diagonal peak pair clearly changes shape between 1 and 5 ps, indicating a shift from diagonal to off-diagonal character.

and the ν = 1 mode is populated. This results in a bleach of the ν = 0 → 1 absorption due to depopulation of the ground state and stimulated emission from ν = 1 → 0, and to a transient ν = 1 → 2 absorption anharmonically shifted to lower energies, giving the characteristic differential absorption profiles of Figure 2. This is usually referred to as a *diagonal* peak pair (pump frequency ≈ probe frequency). If the pumped vibration is coupled to other modes in the molecule, these other modes will respond to the excitation and show *cross-peak* or *off-diagonal* bleach-transient pairs separated by the off-diagonal anharmonicity, which corresponds to the frequency shift of the combination band of the two vibrations. Thus, the distinction between diagonal and off-diagonal signals can be made by analyzing the band shapes and peak positions. 2DIR spectral analysis has been extensively described in several publications, see for example refs 3, 4, 19, and 21.

Figure 2F shows how the a(es) bleach/transient peak pair separation depends on which mode is excited. The diagonal response peak pair (blue) is clearly different to the off-diagonal response (red and black). However, the diagonal a(es) band shape changes with time, evolving into off-diagonal character (green) within 5 ps of excitation. This indicates that the ester C═O stretch modes undergo IVR rapidly to populate spatially

dx.doi.org/10.1021/jp506326u | J. Phys. Chem. B 2014, 118, 11781−11791

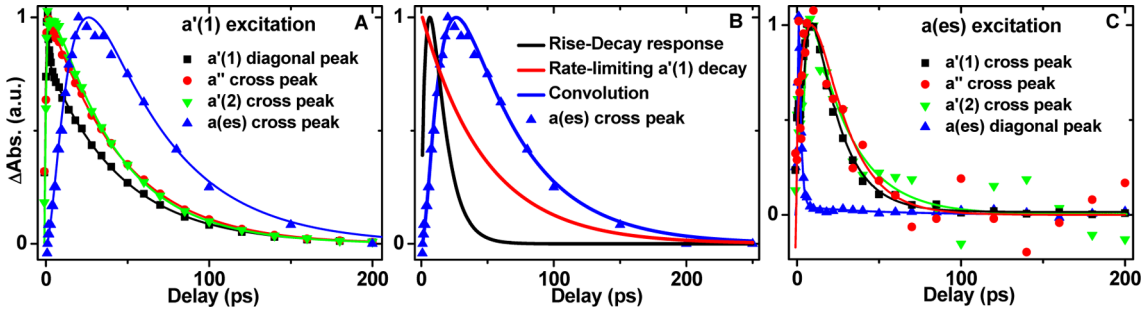

Figure 3. Ground State 2DIR kinetic traces showing the diagonal and cross-peak population dynamics of different vibrations to (A) a′(1) excitation and (C) a(es) excitation. Panel (B) shows the kinetic model used to deconvolute the a(es) cross-peak dynamics from the rate-limiting a′(1) decay (see text for details). Solid lines represent best fits using mono or biexponential decays deconvolved from a Gaussian instrument response function. Fitting parameters are summarized in Table 1.

Table 1. Summary of C≡O and C═O Diagonal and Cross-Peak Lifetimes in Picoseconds from GS2DIR Data[a]

		probe			
		a(es)	a′(2)	a″	a′(1)
pump	a(es)	1.1 ± 0.3 (91%)	(−) 7 ± 3	(−) 8 ± 1	(−) 6 ± 1
		9 ± 2 (9%)	21 ± 3	14 ± 1	15 ± 1
	a″	(−) 14 ± 2	48 ± 4	45 ± 1	(−) 4 ± 2
		40 ± 10			47 ± 4
	a′(1)	(−) 5 ± 1[b]	(−) 3 ± 2	(−) 3 ± 2	0.7 ± 0.5 (42%)
		11 ± 2[b]	46 ± 3	41 ± 3	48 ± 6 (58%)

[a]Kinetic traces were fitted to a sum of exponentials convoluted with a Gaussian instrumental response function which was determined to be between 1.5 and 1.7 ps depending on the experimental conditions. Negative signs in brackets indicate the lifetimes correspond to grow-in of the signals. For bi-exponential decays, relative component contributions are shown in brackets. Quoted lifetimes are averages ±1 standard deviation from several fits of the bleach dynamics of peak pairs, checked against integrated transient band dynamics. [b]Rise−decay deconvolved from the rate-limiting a′(1) decay. See Figure 3B and text for details.

nearby low-frequency modes which are anharmonically coupled to a(es), giving rise to the observed off-diagonal signal.[3]

Investigating the spectral dynamics of intermode coupling provides insight into the mechanisms responsible for these interactions. Figure 3 shows the diagonal and cross-peak dynamics of different modes following a′(1) excitation (A) and a(es) excitation (C). All subsequent kinetic traces were obtained from the bleaches of the peak pairs and fitted to a sum of exponentials convoluted with a Gaussian instrumental response function; Table 1 gives a summary of the obtained lifetimes. Note that these experiments have a time resolution of approximately 1.5 ps (limited by the ca. 12 cm^{-1} fwhm pump requirement), and therefore nothing quantitative can be inferred from kinetic components of <1 ps as these are highly dependent on the width of the instrumental response function used.

Following a′(1) excitation, a″ and a′(2) respond within the instrument response as the three modes share the same ground state.[19,28] For the a′(1) mode, a short, instrument-limited diagonal peak decay component (0.7 ps) is followed by a longer decay (48 ps). The cross-peak dynamics of a″ and a′(2) show a short grow-in followed by a concerted decay (within instrumental error) with a′(1) (Table 1). The off-diagonal band shapes of a″ and a′(2) evolve subtly in the first few ps after a′(1) excitation. This corresponds well to the previously reported subpicosecond population equilibration between a′(1), a″, and a′(2).[26,61] The three modes then decay simultaneously through concerted IVR to lower frequency modes within the molecule with a $(48\ ps)^{-1}$ rate constant.[26,61]

The a(es) cross-peak formed upon a′(1) excitation is clearly delayed, reaching a maximum at t_{max} = 27 ps. This delayed response may arise from the propagation of vibrational energy from the excited C≡O modes through anharmonically coupled low-frequency modes across the molecule.[7,8,62] This VET eventually reaches low-frequency modes that are in spatial proximity to the C═O groups and are anhamonically coupled to a(es), giving rise to the off-diagonal signal observed. However, the apparent 27 ps arrival time of the probed a(es) mode is clearly shorter than the 48 ps vibrational decay lifetime of the pumped a′(1) mode. This response time shorter than the decay of the pumped mode occurs because the 48 ps lifetime of the C≡O stretches is the rate limiting step in this experiment: a′(1) relaxation is slower than subsequent VET across the molecule and equilibration of intramolecular low-frequency modes with the surrounding solvent bath (vibrational cooling). The convolution of the slow a′(1) $\nu = 1$ exponential decay with the probed response dynamics is distorting the off-diagonal a(es) peak kinetics. By deconvolving the a(es) cross-peak dynamics from the slow a′(1) decay, one can extract the response dynamics as if the a′(1) $\nu = 1$ mode was infinitely short-lived.[63] This is shown in Figure 3B. In the black curve, the rise (τ = 5 ps) represents the actual VET rate, and the decay (τ = 11 ps) corresponds to energy equilibration and vibrational cooling to the surrounding solvent bath.[1,64]

When a(es) is excited, the evolution depicted in Figure 2F is observed: an initial diagonal peak pair decays with a 1.1 ps lifetime, giving rise to an off-diagonal signal which decays with a 9 ps lifetime. This shows that the a(es) $\nu = 1$ mode is short-lived (τ = 1.1 ps), quickly undergoing IVR to spatially close lower-frequency modes which couple to a(es). These low-frequency modes then undergo vibrational relaxation on a 9 ps time scale. a′(1), a′(2), and a″ cross-peaks have an

dx.doi.org/10.1021/jp506326u | J. Phys. Chem. B 2014, 118, 11781−11791

appropriately delayed response to a(es) excitation, with grow-in times of approximately 7 ps (arrival time t_{max} = 9 ps). The a′(1), a′(2) and a″ cross-peaks decay over 14−21 ps lifetimes (Table 1), corresponding to energy equilibration and vibrational cooling.

To probe VR and VET processes in the electronic excited state and directly compare them with ground-state behavior, one can use a UV(pump)−IR(pump)−IR(probe) pulse sequence (Figure 1A) in which the 2DIR experiment is preceded by UV excitation which populates the excited state of interest.[21] To perform such experiments on ReCOe, we electronically excite the sample using a 400 nm, ∼50 fs pulse, and then let it relax for 600 ps by which time the vibrationally cooled and fully solvated ^{3}CT (Re/Cl-to-bpy charge transfer) state is fully formed, as is evidenced by lack of spectral evolution in the TRIR spectra.[11,17] We then interrogate the relaxed ^{3}CT state using the IR pump−probe sequence. Figure 4A shows a 1-D slice of an excited state 2DIR (ES2DIR) spectrum upon excitation of the a′(1)* band at 2070 cm^{-1}. Figure 4B shows the vibrational response dynamics, which occur on a strikingly faster time scale than in the ground state.

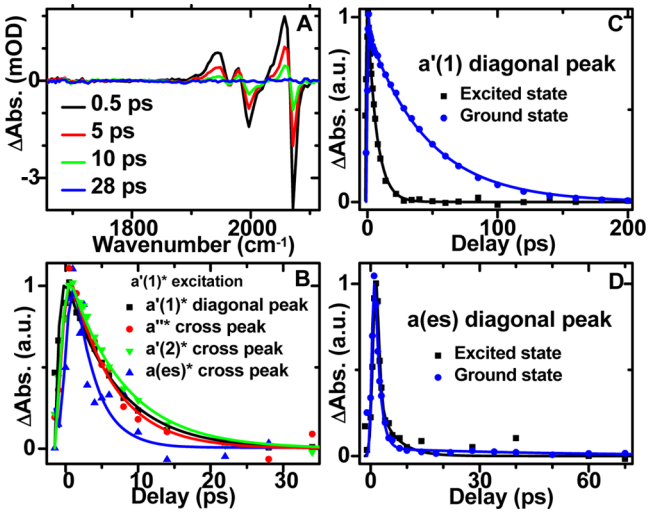

Figure 4. Excited state 2DIR of ReCOe in CD_2Cl_2, with UV pump−IR pump delay t_1 = 600 ps. (A) 1D pump−probe spectra at representative delay times following a′(1)* excitation. (B) Kinetics traces showing the response dynamics of different modes following a′(1)* excitation. (C,D) Comparison of ground (blue) and excited state (black) a′(1) (C) and a(es) (D) diagonal peak dynamics. Solid lines represent best fits using mono- or biexponential decays deconvolved from a Gaussian instrument response function. Fitting parameters are summarized in Table 2

Figure 4 panels C and D compare the excited (black) and ground state (blue) diagonal peak pair dynamics of the a′(1) mode and a(es) mode, respectively. The a′(1)* ν = 1 mode has a lifetime of 6.5 ps, that is, seven times faster than in the ground state (similarly to other C≡O modes, see Table 2). The a(es)* ν = 1 mode decays in 0.7 ps, which is not markedly different to the ground state decay of 1.1 ps, those values being within experimental error of each other. However, the second component of that decay, which corresponds to the relaxation of the anharmonically coupled low-frequency modes in the vicinity of the C═O bonds, is noticeably shorter in the excited state: 3.8 ps compared to 9 ps in the ground state. Correspondingly, the a′(1)* cross-peak response time of 3.4 ps (t_{max} = 4.5 ps) following a(es)* excitation is faster in the excited state. Quantitative information could not be inferred from the a(es)* cross-peak dynamics in response to the excitation of the a′(1)* mode due to a too low signal-to-noise ratio.

The results in the ground state showing a large difference between a(es) and a′(1) IVR rates correspond well with those reported for bis(maleonitriledithiolate)iron(III)nitrosyl[63] where the N═O, directly attached to the Fe center, possesses a much greater vibrational lifetime than C≡N; the observation is rationalized by a lack of transport pathways from the isolated N═O mode which has to couple to low-frequency Fe−N modes to transfer energy to the rest of the molecule. In ReCOe, the multitude of IVR and VET pathways originating from the ester C═O group to spatially close medium and low-frequency modes allow for rapid energy transfer, whereas the C≡O modes are insulated by the metal center. The fact that the vibrational lifetime of C≡O modes in the excited state are significantly shortened points to the presence of alternative vibrational coupling processes for the deactivation of C≡O, which are discussed in more detail below.

Solvent Dependence of Vibrational Relaxation Dynamics in ReCOe. Figure 5 presents FTIR, TRIR, and 2DIR data for ReCOe in three solvents of different polarity, namely CH_2Cl_2 (black, ε = 8.9), toluene (red, ε = 2.4), and MeCN (blue, ε = 37.5). The parameters used to obtain best fits for the a′(1) and a′(1)* deactivation are detailed in Table 3. In the ground state (Figure 5C), a′(1) ν = 1 relaxation rates exhibit a significant dependence on the solvent. In CH_2Cl_2, the lifetime of the a′(1) ν = 1 mode is 51 ps, which is the same as in CD_2Cl_2, within instrumental error. In the considerably more polar MeCN, the lifetime is reduced to 31 ps. In nonpolar

Table 2. Summary of C≡O and C═O Diagonal and Cross-Peak Lifetimes (in Picoseconds) from ES2DIR Data[a]

		probe			
		a(es)*	a′(2)*	a″*	a′(1)*
pump	a(es)*	0.7 ± 0.2 (81%) 3.8 ± 0.9 (19%)	*b*	*b*	(−) 3.4 ± 2 13 ± 2
	a′(1)*	(−) 0.1 ± 1[b] 5 ± 2	7.4 ± 0.2	5.8 ± 0.2	0.3 ± 0.2 (49%) 6.5 ± 0.8 (51%)

[a]Kinetic traces were fitted to a sum of exponentials convoluted with a Gaussian instrumental response function which was determined to be between 1.5 and 1.7 ps depending on the experimental conditions. Negative signs in brackets indicate that the lifetimes correspond to grow-in of the signal. For bi-exponential decays, relative component contributions are shown in brackets. Quoted lifetimes are averages ±1 standard deviation from several fits of the bleach dynamics of peak pairs, checked against integrated transient band dynamics. [b]S/N ratios for these responses were too low to obtain satisfactory fits.

dx.doi.org/10.1021/jp506326u | J. Phys. Chem. B 2014, 118, 11781−11791

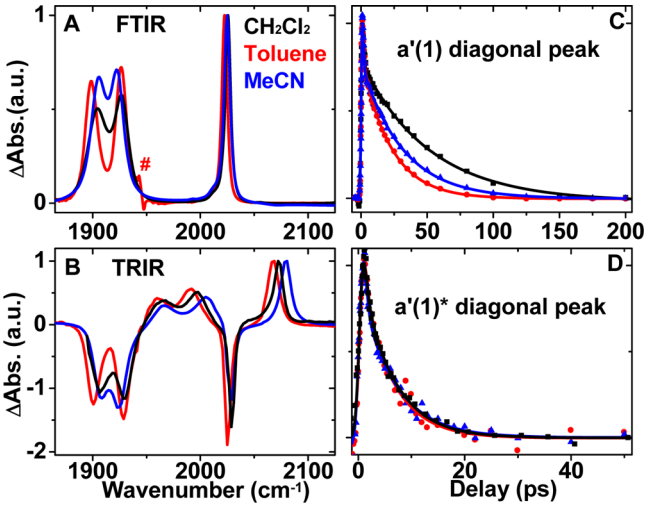

Figure 5. FTIR (A), TRIR at 600 ps (B), GS2DIR (C), and ES2DIR (D) of ReCOe in CH_2Cl_2 (black), toluene (red), and MeCN (blue). The number sign (#) denotes a toluene absorbance band position. C and D show the different lifetimes of the a′(1) and a′(1)* $\nu = 1$ mode in different solvents. Solid lines represent best fits using biexponential decays deconvolved from a 1.5 ps Gaussian instrument response function. Fitting parameters are summarized in Table 3

Table 3. Summary of Lifetimes from the Fitting of a′(1) (Ground State) and a′(1)* (Excited State) Diagonal Peaks in Different Solvents[a]

solvent (ε)	$\tau_{a'(1)}$ (ps) ground state	$\tau_{a'(1)^*}$ (ps) excited state
CD_2Cl_2 (8.9)	0.7 ± 0.5	0.3 ± 0.1
	48 ± 6	6.5 ± 0.8
CH_2Cl_2 (8.9)	0.4 ± 0.3	0.3 ± 0.2
	51 ± 8	6.6 ± 0.5
Toluene (2.4)	1.3 ± 0.4	0.4 ± 0.3
	22 ± 1	5.6 ± 0.1
MeCN (37.5)	0.5 ± 0.1	0.4 ± 0.3
	31 ± 1	6.4 ± 0.2

[a]All fitting procedures used an instrumental response function of 1.5 ps. Quoted lifetimes are averages ±1 standard deviation from several fits of the bleach recovery dynamics, checked against integrated transient band dynamics.

toluene the lifetime is further reduced to 22 ps. We do not discuss the response of the a(es) mode, as the corresponding band is partially obscured by solvent absorption, making it difficult to extract the kinetic information.

In the excited state, the a′(1)* $\nu = 1$ mode again relaxes much faster than in the ground state in all solvents, but rather surprisingly its decay shows almost no solvent-dependence (Table 3). The lifetimes in CD_2Cl_2, CH_2Cl_2, and MeCN are all approximately 6.5 ps, while in toluene the decay is marginally faster at 5.6 ps.

DISCUSSION

The main findings of this study may be summarized as follows: (i) Vibrational relaxation and energy transfer in the lowest ^{3}CT excited state of ReCOe is substantially faster than in its ground electronic state. (ii) Vibrational relaxation rates are solvent-dependent in the ground state but solvent insensitive in the excited state.

To rationalize these results, several concepts related to intermolecular frequency and charge fluctuations, resonant energy transfer, intramolecular electrostatic interactions, and anharmonic coupling in transition metal carbonyls are needed.

Pathways for Vibrational Relaxation. Figure 6 depicts the typical pathways for VR and VET applicable to polyatomic

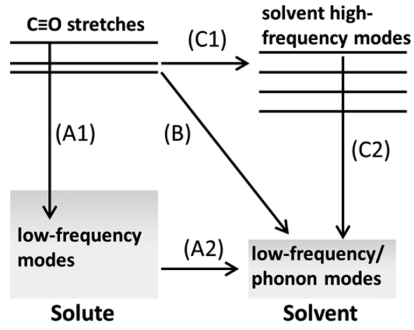

Figure 6. Depiction of typical pathways for VR and VET from the high-frequency C≡O modes of ReCOe. The vibrationally excited solute may undergo IVR (A1) and subsequently transfer energy to the surrounding solvent phonon bath (A2, vibrational cooling); it may also directly couple to low-frequency solvent modes (B) if this cooling process is kinetically competitive with IVR. In cases where the solvent has high-frequency modes in the same frequency range as the C≡O stretches of the solute, resonant energy transfer to the solvent may occur (C1), followed by IVR in the solvent (C2).[58,65]

molecules in solution.[58,65] VET across the molecule from C≡O to low-frequency modes in spatial proximity to C═O and vice versa occurs primarily through intramolecular anharmonic coupling—it has been shown that transition-dipole coupling is inadequate to account for such long-distance VET in various systems, whereas strong mechanical mode coupling accurately represents the structural dependence of these processes.[3,7,8,20,26] The excited mode undergoes IVR to anharmonically coupled low-frequency modes (process A1 in Figure 6), and the energy propagates through the molecule until it reaches modes in the vicinity of the probed vibration, giving rise to off-diagonal signals. VET rates are highly dependent on the IVR rates of the source and intermediate modes, the number of modes coupled to the source mode and involved in the energy transfer, and the kinetic competition between equilibration with the solvent bath (A2 and B) and IVR.

An alternative VR pathway is through resonant energy transfer to the solvent (C1). Indeed, it has been shown that water molecules can speed up the C≡O stretch relaxation process significantly in metal carbonyls as its libration-bend combination band provides a resonant channel for intermolecular energy transfer, and the extensive hydrogen-bonding network provides a large density of low-frequency states in the solvent bath for solvent–solute equilibration.[58] Toluene possesses several combination bands in the 1720–2000 cm^{-1} region that are resonant with the CO stretch bands of ReCOe and therefore provide a resonant transfer pathway, which can explain the faster decay of the ground state a′(1) mode in toluene than in other solvents. Assuming the deactivation rate of the a′(1) mode without resonant transfer is similar in toluene as it is in CH_2Cl_2, that is, $(51\ ps)^{-1}$, the 22 ps a′(1) lifetime in toluene implies a $(39\ ps)^{-1}$ rate constant for intermolecular resonant energy transfer.

Charge and Frequency Fluctuations. On subpicosecond time scales, quantum dynamical effects such as vibrational dephasing and vibrational coherences will be strongly affected

dx.doi.org/10.1021/jp506326u | J. Phys. Chem. B 2014, 118, 11781–11791

by fluctuating fields.[66−68] For example, it has been shown that in water, instantaneous vibrational frequency shifts are directly proportional to the liquid's electric field, and that fluctuations in the local and collective electric fields destroy vibrational coherence.[67] Similarly, solvent-induced and intramolecular frequency and charge fluctuations allow for wider structural fluctuations of the solute, increasing coupling strength between high and low-frequency modes through the sampling of optimal coupling geometries.[69−71] It has been shown that water can speed up the C≡O relaxation process in metal carbonyls not only through the aforementioned resonant energy transfer but also through solvent-enhanced intramolecular coupling in the presence of a rapidly fluctuating local electric field produced by water's large dipole and fast reorientation dynamics.[58]

Rather counterintuitively, the total dipole moment of ReCOe in the ground state is larger than in the ^{3}CT excited state.[72] The DFT-calculated total dipole moments are 15.5D in the ground state and 5.8D in the lowest triplet state in CH_2Cl_2. The faster decay of the ground state a′(1) mode in the polar, aprotic solvent MeCN (31 ps lifetime compared to 51 ps in CH_2Cl_2, Table 3) can thus be rationalized through solvent-enhanced intramolecular coupling similar to that found for metal carbonyls in water,[58] although the effect is far less dramatic in this case.

The authors of a thorough analysis of the excited state dynamics of a series of similar Re(I) diimine tricarbonyl complexes in different solvents[17] suggested that the solute and local solvent molecules form a strongly interacting supramolecular cluster, with solvent molecules probably inserted between the ligands. This has two important consequences in the context of this study. First, each solvent molecule will experience a different electrostatic environment. Thus, the frequency fluctuations across different parts of the cluster may not be correlated and have very different effects on the vibrational dynamics of various intramolecular modes. Although the ^{3}CT state has a lower overall average dipole, some local solvent−solute electrostatic interactions may be greater following charge redistribution in the excited state. Indeed, the broadening of the IR bands in the ^{3}CT state may be a direct indication of the larger charge and frequency fluctuations experienced by the CO bonds.[57]

The close ligand-solvent proximity and strong dipole interactions may also provide an alternative, intermolecular VET pathway. For intramolecular through-bond energy transfer from one end of ReCOe to the other, all energy has to pass through a central heavy metal atom, which is known to insulate and slow down VR considerably.[73] VR and VET rates could therefore largely be dictated by this Re "bottleneck". Accelerated vibrational dynamics may occur in the excited state if the insulating Re atom constraint can be circumvented by transferring energy through the low-frequency modes of the solvent molecules inserted between the ligands, which then couple back to the solute.

However, both of these hypotheses (stronger frequency/charge fluctuations in the excited state, and intermolecular VET) are incompatible with the solvent-independent vibrational dynamics in the excited state (Figure 5B). The solvents have vastly different polarities, as well as varying thermal conductivity, viscosity, and dielectric relaxation rates,[74,75] yet these have no effect on the a′(1)* relaxation rate. The slightly faster decay rate in toluene is rationalized through a minor resonant energy transfer pathway—the above calculated rate constant $(39\ \text{ps})^{-1}$ for resonant VET reduces the 6.5 ps lifetime, measured for a′(1)* deactivation in CH_2Cl_2, CD_2Cl_2, and MeCN, to 5.6 ps, which is precisely the measured lifetime in toluene. This solvent-insensitivity suggests that a predominantly intramolecular effect is responsible for the considerable acceleration of vibrational relaxation in the excited state of ReCOe.

Bonding and Intramolecular Electrostatic Interactions in Transition Metal Carbonyls. The dominant bonding model for transition metal carbonyl revolves around a synergistic CO → metal σ-donation and metal → CO π back-donation.[76] The vibrational frequencies of the CO modes are highly sensitive to this bonding interaction, and it has been shown that π back-donation is the main feature responsible for lowering the CO frequencies to below that of free CO (2143 cm^{-1})[76] in classical transition metal carbonyls. Upon photoexcitation of ReCOe, the shift of electron density away from the metal center toward the bpy unit reduces π back-donation to the antibonding orbital, resulting in a shortening of CO bonds, lengthening of Re−C bonds, and increased CO frequencies (Figure 1D).[51,52,77]

Several studies have shown that the extent of π back-donation is also the major factor in determining C≡O vibrational relaxation rates in metal carbonyls, as it facilitates intramolecular anharmonic coupling of the CO modes to surrounding low-frequency modes. Thus, the frequency and vibrational lifetimes are both inversely proportional to the extent of π back-donation into the π^* orbital of CO.[30,78−80] Assuming that this model is applicable to the ^{3}CT state of ReCOe, less π back-donation should result in increased frequencies and increased vibrational lifetimes; however *decreased* vibrational lifetimes are observed (Table 3). This contradiction suggests that another significant interaction must be responsible for the observed decreased lifetime of the a′(1)* mode.

Electrostatic interactions have been shown to play a significant role in the binding energetics of transition metal carbonyls, especially in cationic forms of the metal center.[76,81−83] Thus, in the ^{3}CT state with the rhenium atom formally partially oxidized, charge interactions between the CO and metal center are expected to play an important role on intramolecular coupling. Indeed, Mulliken and Merz−Kollman population analyses[84,85] reveal a stronger dipole over the O≡C−Re−N region of the molecule in the triplet state than in the singlet ground state (see Supporting Information), so that while the total dipole is smaller, the specific bond dipoles relevant to intramolecular C≡O mode deactivation are larger in ^{3}CT. We propose that these intramolecular electrostatic interactions are at least partially responsible for the much-increased rates of vibrational relaxation of the a′(1)* mode.

This hypothesis may be further supported by the data shown in Figure 4D (and Tables 1 and 2), which indicate that there is little detectable difference in the a(es) ν = 1 mode lifetime between ground and excited state, which would not be vastly affected by electrostatic interactions between Re and the C≡O ligands; however, energy transfer out of spatially close low-frequency modes such as bpy-localized modes is accelerated in the excited state. Thermodynamically unfavorable energy transfer steps are likely to slow down VET or not occur at all. For example if the transfer from Re−N modes to Re−C modes is energetically uphill, it may slow down a(es) → a′(1) VET, although the latter may still be allowed through scattering mechanisms involving phonon modes of the solvent bath providing the excess energy required.[86] Stronger intramolecular

dx.doi.org/10.1021/jp506326u | J. Phys. Chem. B 2014, 118, 11781−11791

charge interactions in the ^{3}CT state could help overcome such structural barriers through local electrostatic rather than mechanical coupling and would explain the substantial differences in a′(1) ν = 1 lifetime between the ground and excited state.

To shed light on the exact mechanism through which vibrational relaxation is facilitated in the excited state of such transition metal carbonyl complexes requires further studies where the solvent is more drastically varied, for example using ionic liquids[17,72] or performing these experiments in the gas phase,[87] as well as systematically varying ligands to influence the nature and ordering of the excited states from MLCT to ligand-to-ligand CT or intraligand triplet states,[22,56] which would consequently change bonding and electrostatic interactions.

CONCLUSIONS

Using frequency-domain 2DIR spectroscopy, we have investigated the ground and excited state vibrational relaxation and energy transfer dynamics of Re(Cl)(CO)$_3$(4,4′-diethylester-2,2′-bipyridine) in solution, where two IR reporters are ca. 9 Å apart and positioned across the metal center. The results in the ground state can be rationalized assuming that IVR and VET occur primarily through intramolecular mechanical anharmonic coupling assisted by solvent-induced fluctuations. As such, VR and VET rates are in part dictated by structural constraints in the molecule, such as the central heavy Re atom acting as a bottleneck through which all long-range intramolecular VET has to go. In the lowest triplet excited state of primarily metal-to-ligand CT character, up to eight times faster VR rates are observed. Although ground state vibrational dynamics are solvent-dependent, the C≡O stretch lifetimes in the ^{3}CT state are surprisingly solvent-insensitive. This observation suggests that purely intramolecular effects are responsible for the rapid vibrational deactivation of C≡O modes in the excited state. On the basis of several studies,[30,78−80] the reduced π back-donation in the MLCT excited state would be expected to slow down rather than speed up VR. We thus propose that intramolecular electrostatic rather than π-bonding interactions between the C≡O and partially oxidized metal center are responsible for increased vibrational coupling in the excited state, overcoming structural and thermodynamic barriers which slow down C≡O IVR in the ground state. This route of intramolecular excess energy redistribution may play a determining role in photoinduced excited state processes in ReCOe. Since the latter can serve as a model for diverse charge-transfer transition metal complexes of great importance to electron and energy transfer-based applications such as solar energy conversion, and given the significance of vibrational quantum state in electron transfer rates and of vibronic coupling facilitating nonequilibrium processes in transition metal complexes, this effect may be of significance for photoinduced processes in transition metal complexes in general.

ASSOCIATED CONTENT

Supporting Information

Details on anharmonic frequency calculations, electron density distribution maps, calculated Mulliken and Merz−Kollman charges, and Cartesian coordinates for the optimized lowest singlet and triplet states of ReCOe. The full details of X-ray crystallographic studies. This material is available free of charge via the Internet at http://pubs.acs.org.

Accession Codes

CCDC deposition number for X-ray structure of ReCOe: 1008868.

AUTHOR INFORMATION

Corresponding Authors

*E-mail: a.meijer@sheffield.ac.uk.
*E-mail: julia.weinstein@sheffield.ac.uk.

Notes

The authors declare no competing financial interest.

ACKNOWLEDGMENTS

We would like to thank Dr Jan Helbing and Dr Paul Donaldson for helpful discussions. We thank the EPSRC, E-Futures DTC, Shine DTC, the University of Sheffield, and the STFC (program access to the Laser for Science facility) for financial support. All calculations were performed on the "Jupiter" cluster of the Theoretical Chemistry Group of the University of Sheffield.

REFERENCES

(1) Wang, Z.; Pakoulev, A.; Dlott, D. D. Watching Vibrational Energy Transfer in Liquids with Atomic Spatial Resolution. *Science* **2002**, *296*, 2201−2203.

(2) Elsaesser, T.; Kaiser, W. Vibrational and Vibronic Relaxation of Large Polyatomic Molecules in Liquids. *Annu. Rev. Phys. Chem.* **1991**, *42*, 83−107.

(3) Rubtsov, I. V.; Hochstrasser, R. M. Vibrational Dynamics, Mode Coupling, and Structural Constraints for Acetylproline-NH$_2$. *J. Phys. Chem. B* **2002**, *106*, 9165−9171.

(4) Hamm, P.; Zanni, M. *Concepts and Methods of 2D Infrared Spectroscopy*; Cambridge University Press: UK, 2011.

(5) Hamm, P.; Lim, M.; Hochstrasser, R. M. Structure of the Amide I Band of Peptides Measured by Femtosecond Nonlinear-Infrared Spectroscopy. *J. Phys. Chem. B* **1998**, *102*, 6123−6138.

(6) Hochstrasser, R. M. Two-Dimensional Spectroscopy at Infrared and Optical Frequencies. *Proc. Natl. Acad. Sci. U.S.A.* **2007**, *104*, 14190−14196.

(7) Kurochkin, D. V.; Naraharisetty, S. R. G.; Rubtsov, I. V. A Relaxation-Assisted 2D IR Spectroscopy Method. *Proc. Natl. Acad. Sci. U.S.A.* **2007**, *104*, 14209−14214.

(8) Rubtsov, I. V. Relaxation-Assisted Two-Dimensional Infrared (RA 2DIR) Method: Accessing Distances over 10 Å and Measuring Bond Connectivity Patterns. *Acc. Chem. Res.* **2009**, *42*, 1385−1394.

(9) Schrauben, J. N.; Dillman, K. L.; Beck, W. F.; McCusker, J. K. Vibrational Coherence in the Excited State Dynamics of Cr(acac)$_3$: Probing the Reaction Coordinate for Ultrafast Intersystem Crossing. *Chem. Sci.* **2010**, *1*, 405−410.

(10) Bressler, C.; Milne, C.; Pham, V.-T.; ElNahhas, A.; van der Veen, R. M.; Gawelda, W.; Johnson, S.; Beaud, P.; Grolimund, D.; Kaiser, M.; et al. Femtosecond XANES Study of the Light-Induced Spin Crossover Dynamics in an Iron(II) Complex. *Science* **2009**, *323*, 489−492.

(11) Cannizzo, A.; Blanco-Rodríguez, A. M.; El Nahhas, A.; Sebera, J.; Zális, S.; Vlcek, A.; Chergui, M. Femtosecond Fluorescence and Intersystem Crossing in Rhenium(I) Carbonyl−Bipyridine Complexes. *J. Am. Chem. Soc.* **2008**, *130*, 8967−8974.

(12) Van der Veen, R. M.; Cannizzo, A.; van Mourik, F.; Vlček, A.; Chergui, M. Vibrational Relaxation and Intersystem Crossing of Binuclear Metal Complexes in Solution. *J. Am. Chem. Soc.* **2011**, *133*, 305−315.

(13) Damrauer, N.; Cerullo, G.; Yeh, A.; Boussie, T.; Shank, C.; McCusker, J. Femtosecond Dynamics of Excited-State Evolution in [Ru(bpy)$_3$]$^{2+}$. *Science* **1997**, *275*, 54−57.

(14) Ardo, S.; Meyer, G. J. Photodriven Heterogeneous Charge Transfer with Transition-Metal Compounds Anchored to TiO_2 Semiconductor Surfaces. *Chem. Soc. Rev.* **2009**, *38*, 115−164.
(15) Spears, K. G.; Wen, X.; Zhang, R. Electron Transfer Rates from Vibrational Quantum States. *J. Phys. Chem.* **1996**, *100*, 10206−10209.
(16) Barbara, P. F.; Walker, G. C.; Smith, T. P. Vibrational Modes and the Dynamic Solvent Effect in Electron and Proton Transfer. *Science* **1992**, *256*, 975−981.
(17) El Nahhas, A.; Cannizzo, A.; van Mourik, F.; Blanco-Rodríguez, A. M.; Zális, S.; Vlcek, A.; Chergui, M. Ultrafast Excited-State Dynamics of $[Re(L)(CO)_3(bpy)]n$ Complexes: Involvement of the Solvent. *J. Phys. Chem. A* **2010**, *114*, 6361−6369.
(18) Lynch, M. S.; Van Kuiken, B. E.; Daifuku, S. L.; Khalil, M. On the Role of High-Frequency Intramolecular Vibrations in Ultrafast Back-Electron Transfer Reactions. *J. Phys. Chem. Lett.* **2011**, *2*, 2252−2257.
(19) Hunt, N. T. 2D-IR Spectroscopy: Ultrafast Insights into Biomolecule Structure and Function. *Chem. Soc. Rev.* **2009**, *38*, 1837−1848.
(20) Müller-Werkmeister, H. M.; Li, Y.-L.; Lerch, E.-B. W.; Bigourd, D.; Bredenbeck, J. Ultrafast Hopping from Band to Band: Assigning Infrared Spectra Based on Vibrational Energy Transfer. *Angew. Chem., Int. Ed. Engl.* **2013**, *52*, 6214−6217.
(21) Bredenbeck, J.; Helbing, J.; Kolano, C.; Hamm, P. Ultrafast 2D-IR Spectroscopy of Transient Species. *ChemPhysChem* **2007**, *8*, 1747−1756.
(22) El Nahhas, A.; Consani, C.; Blanco-Rodríguez, A. M.; Lancaster, K. M.; Braem, O.; Cannizzo, A.; Towrie, M.; Clark, I. P.; Zális, S.; Chergui, M.; et al. Ultrafast Excited-State Dynamics of rhenium(I) Photosensitizers $[Re(Cl)(CO)_3(N,N)]$ and $[Re(imidazole)(CO)_3(N,N)]^+$: Diimine Effects. *Inorg. Chem.* **2011**, *50*, 2932−2943.
(23) Xiong, W.; Laaser, J. E.; Paoprasert, P.; Franking, R. A.; Hamers, R. J.; Gopalan, P.; Zanni, M. T. Transient 2D IR Spectroscopy of Charge Injection in Dye-Sensitized Nanocrystalline Thin Films. *J. Am. Chem. Soc.* **2009**, *131*, 18040−18041.
(24) Paoprasert, P.; Laaser, J. E.; Xiong, W.; Franking, R. A.; Hamers, R. J.; Zanni, M. T.; Schmidt, J. R.; Gopalan, P. Bridge-Dependent Interfacial Electron Transfer from Rhenium−Bipyridine Complexes to TiO_2 Nanocrystalline Thin Films. *J. Phys. Chem. C* **2010**, *114*, 9898−9907.
(25) Hawecker, J.; Lehn, J.; Ziessel, R. Efficient Photochemical Reduction of CO_2 to CO by Visible Light Irradation of Systems Containing $Re(bipy)(CO)_3X$ or $Ru(bipy)_3^{2+}$-CO_2^+ Combinations as Homogeneous Catalysts. *J. Chem. Soc. Chem. Commun.* **1983**, 536−538.
(26) Anfuso, C. L.; Ricks, A. M.; Rodriguez-Cordoba, W.; Lian, T. Ultrafast Vibrational Relaxation Dynamics of a Rhenium Bipyridyl CO_2-Reduction Catalyst at a Au Electrode Surface Probed by Time-Resolved Vibrational Sum Frequency Generation Spectroscopy. *J. Phys. Chem. C* **2012**, *116*, 26377−26384.
(27) Shih, C.; Museth, A. K.; Abrahamsson, M.; Blanco-Rodriguez, A. M.; Di Bilio, A. J.; Sudhamsu, J.; Crane, B. R.; Ronayne, K. L.; Towrie, M.; Vlcek, A.; et al. Tryptophan-Accelerated Electron Flow through Proteins. *Science* **2008**, *320*, 1760−1762.
(28) Baiz, C. R.; McRobbie, P. L.; Anna, J. M.; Geva, E.; Kubarych, K. J. Two-Dimensional Infrared Spectroscopy of Metal Carbonyls. *Acc. Chem. Res.* **2009**, *42*, 1395−1404.
(29) Bredenbeck, J.; Helbing, J.; Hamm, P. Transient Two-Dimensional Infrared Spectroscopy: Exploring the Polarization Dependence. *J. Chem. Phys.* **2004**, *121*, 5943−5957.
(30) Rosenfeld, D. E.; Gengeliczki, Z.; Smith, B. J.; Stack, T. D. P.; Fayer, M. D. Structural Dynamics of a Catalytic Monolayer Probed by Ultrafast 2D IR Vibrational Echoes. *Science* **2011**, *334*, 634−639.
(31) Bredenbeck, J.; Helbing, J.; Hamm, P. Labeling Vibrations by Light: Ultrafast Transient 2D-IR Spectroscopy Tracks Vibrational Modes during Photoinduced Charge Transfer. *J. Am. Chem. Soc.* **2004**, *126*, 990−991.
(32) Bonner, G. M.; Ridley, A. R.; Ibrahim, S. K.; Pickett, C. J.; Hunt, N. T. Probing the Effect of the Solution Environment on the Vibrational Dynamics of an Enzyme Model System with Ultrafast 2D-IR Spectroscopy. *Faraday Discuss.* **2010**, *145*, 429−442.
(33) Kaziannis, S.; Wright, J. A.; Candelaresi, M.; Kania, R.; Greetham, G. M.; Parker, A. W.; Pickett, C. J.; Hunt, N. T. The Role of CN and CO Ligands in the Vibrational Relaxation Dynamics of Model Compounds of the [FeFe]-Hydrogenase Enzyme. *Phys. Chem. Chem. Phys.* **2011**, *13*, 10295−10305.
(34) Bredenbeck, J.; Helbing, J.; Hamm, P. Solvation beyond the Linear Response Regime. *Phys. Rev. Lett.* **2005**, *95*, 083201.
(35) Stewart, A. I.; Wright, J. A.; Greetham, G. M.; Kaziannis, S.; Santabarbara, S.; Towrie, M.; Parker, A. W.; Pickett, C. J.; Hunt, N. T. Determination of the Photolysis Products of [FeFe]hydrogenase Enzyme Model Systems Using Ultrafast Multidimensional Infrared Spectroscopy. *Inorg. Chem.* **2010**, *49*, 9563−9573.
(36) Kania, R.; Stewart, A. I.; Clark, I. P.; Greetham, G. M.; Parker, A. W.; Towrie, M.; Hunt, N. T. Investigating the Vibrational Dynamics of a 17e(−) Metallocarbonyl Intermediate Using Ultrafast Two Dimensional Infrared Spectroscopy. *Phys. Chem. Chem. Phys.* **2010**, *12*, 1051−1063.
(37) Anna, J. M.; Baiz, C. R.; Ross, M. R.; McCanne, R.; Kubarych, K. J. Ultrafast Equilibrium and Non-equilibrium Chemical Reaction Dynamics Probed with Multidimensional Infrared Spectroscopy. *Int. Rev. Phys. Chem.* **2012**, *31*, 367−419.
(38) Baiz, C. R.; McCanne, R.; Kubarych, K. J. Structurally Selective Geminate Rebinding Dynamics of Solvent-Caged Radicals Studied with Nonequilibrium Infrared Echo Spectroscopy. *J. Am. Chem. Soc.* **2009**, *131*, 13590−13591.
(39) Baiz, C. R.; Nee, M. J.; McCanne, R.; Kubarych, K. J. Ultrafast Nonequilibrium Fourier-Transform Two-Dimensional Infrared Spectroscopy. *Opt. Lett.* **2008**, *33*, 2533−2535.
(40) Baiz, C. R.; McCanne, R.; Nee, M. J.; Kubarych, K. J. Orientational Dynamics of Transient Molecules Measured by Nonequilibrium Two-Dimensional Infrared Spectroscopy. *J. Phys. Chem. A* **2009**, *113*, 8907−8916.
(41) Greetham, G.; Burgos, P.; Cao, Q.; Clark, I.; Codd, P.; Farrow, R.; George, M.; Kogimtzis, M.; Matousek, P.; Parker, A.; et al. ULTRA: A Unique Instrument for Time-Resolved Spectroscopy. *Appl. Spectrosc.* **2010**, *64*, 1311−1319.
(42) Hunt, N. T.; Greetham, G. M.; Towrie, M.; Parker, A. W.; Tucker, N. P. Relationship between Protein Structural Fluctuations and Rebinding Dynamics in Ferric Haem Nitrosyls. *Biochem. J.* **2011**, *433*, 459−468.
(43) Frisch, M. J.; Trucks, G. W.; Schlegel, H. B.; Scuseria, G. E.; M. A. Robb, J.; Cheeseman, R.; Scalmani, G.; Barone, V.; Mennucci, B.; Petersson, G. A.; et al. Gaussian 09, Revision A.2, 2009.
(44) Whaley, R. C.; Petitet, A. Minimizing Development and Maintenance Costs in Supporting Persistently Optimized BLAS. *Software Pract. Exp.* **2005**, *35*, 101−121.
(45) Becke, A. D. Density-Functional Thermochemistry. III. The Role of Exact Exchange. *J. Chem. Phys.* **1993**, *98*, 5648−5652.
(46) McLean, A. D.; Chandler, G. S. Contracted Gaussian Basis Sets for Molecular Calculations. I. Second Row Atoms, $Z = 11−18$. *J. Chem. Phys.* **1980**, *72*, 5639−5648.
(47) Cao, X.; Dolg, M. Valence Basis Sets for Relativistic Energy-Consistent Small-Core Lanthanide Pseudopotentials. *J. Chem. Phys.* **2001**, *115*, 7348−7355.
(48) Foxon, S. P.; Green, C.; Walker, M. G.; Wragg, A.; Adams, H.; Weinstein, J. A.; Parker, S. C.; Meijer, A. J. H. M.; Thomas, J. A. Synthesis, Characterization, and DNA Binding Properties of Ruthenium(II) Complexes Containing the Redox Active Ligand Benzo[i]dipyrido[3,2-a:2′,3′-C]phenazine-11,16-quinone. *Inorg. Chem.* **2012**, *51*, 463−471.
(49) Best, J.; Sazanovich, I. V.; Adams, H.; Bennett, R. D.; Davies, E. S.; Meijer, A. J. H. M.; Towrie, M.; Tikhomirov, S. A.; Bouganov, O. V.; Ward, M. D.; et al. Structure and Ultrafast Dynamics of the Charge-Transfer Excited State and Redox Activity of the Ground State of Mono- and Binuclear Platinum(II) Diimine Catecholate and Bis-Catecholate Complexes: A Transient Absorption, TRIR, DFT, and Electrochemical Study. *Inorg. Chem.* **2010**, *49*, 10041−10056.

(50) Mennucci, B.; Tomasi, J. Continuum Solvation Models: A New Approach to the Problem of Solute's Charge Distribution and Cavity Boundaries. *J. Chem. Phys.* **1997**, *106*, 5151−5158.
(51) Dattelbaum, D. M.; Omberg, K. M.; Schoonover, J. R.; Martin, R. L.; Meyer, T. J. Application of Time-Resolved Infrared Spectroscopy to Electronic Structure in Metal-to-Ligand Charge-Transfer Excited States. *Inorg. Chem.* **2002**, *41*, 6071−6079.
(52) Butler, J. M.; George, M. W.; Schoonover, J. R.; Dattelbaum, D. M.; Meyer, T. J. Application of Transient Infrared and near Infrared Spectroscopy to Transition Metal Complex Excited States and Intermediates. *Coord. Chem. Rev.* **2007**, *251*, 492−514.
(53) Kuimova, M. K.; Alsindi, W. Z.; Blake, A. J.; Davies, E. S.; Lampus, D. J.; Matousek, P.; Mcmaster, J.; Parker, A. W.; Towrie, M.; Sun, X.-Z.; et al. Probing the Solvent Dependent Photophysics of Fac-$[Re(CO)_3(dppz\text{-}X_2)Cl]$ (dppz-X_2 = 11,12-X_2-dipyrido[3,2-a:2′,3′-C]-phenazine); X = CH_3, H, F, Cl, CF_3). *Inorg. Chem.* **2008**, *47*, 9857−9869.
(54) George, M. W.; Turner, J. J. Excited States of Transition Metal Complexes Studied by Time-Resolved Infrared Spectroscopy. *Coord. Chem Rev.* **1998**, *177*, 201−217.
(55) Weinstein, J. A.; Grills, D. C.; Towrie, M.; Matousek, P.; Parker, A. W.; George, M. W. Picosecond Time-Resolved Infrared Spectroscopic Investigation of Excited State Dynamics in a PtII Diimine Chromophore. *Chem. Commun. (Cambridge)* **2002**, *1*, 382−383.
(56) Yue, Y.; Grusenmeyer, T.; Ma, Z.; Zhang, P.; Pham, T. T.; Mague, J. T.; Donahue, J. P.; Schmehl, R. H.; Beratan, D. N.; Rubtsov, I. V. Evaluating the Extent of Intramolecular Charge Transfer in the Excited States of Rhenium(I) Donor−Acceptor Complexes with Time-Resolved Vibrational Spectroscopy. *J. Phys. Chem. B* **2013**, *117*, 15903−15916.
(57) Woys, A. M.; Mukherjee, S. S.; Skoff, D. R.; Moran, S. D.; Zanni, M. T. A Strongly Absorbing Class of Non-natural Labels for Probing Protein Electrostatics and Solvation with FTIR and 2D IR Spectroscopies. *J. Phys. Chem. B* **2013**, *117*, 5009−5018.
(58) King, J. T.; Ross, M. R.; Kubarych, K. J. Water-Assisted Vibrational Relaxation of a Metal Carbonyl Complex Studied with Ultrafast 2D-IR. *J. Phys. Chem. B* **2012**, *116*, 3754−3759.
(59) King, J. T.; Anna, J. M.; Kubarych, K. J. Solvent-Hindered Intramolecular Vibrational Redistribution. *Phys. Chem. Chem. Phys.* **2011**, *13*, 5579−5583.
(60) Liard, D. J.; Busby, M.; Matousek, P.; Towrie, M.; Vlcek, A. Picosecond Relaxation of ^{3}MLCT Excited States of $[Re(Etpy)(CO)_3(dmb)]$+ and $[Re(Cl)(CO)_3(bpy)]$ as Revealed by Time-Resolved Resonance Raman, UV−vis, and IR Absorption Spectroscopy. *J. Phys. Chem. A* **2004**, *108*, 2363−2369.
(61) Ricks, A. M.; Anfuso, C. L.; Rodríguez-Córdoba, W.; Lian, T. Vibrational Relaxation Dynamics of Catalysts on TiO_2 Rutile (110) Single Crystal Surfaces and Anatase Nanoporous Thin Films. *Chem. Phys.* **2013**, *422*, 264−271.
(62) Kasyanenko, V. M.; Tesar, S. L.; Rubtsov, G. I.; Burin, A. L.; Rubtsov, I. V. Structure Dependent Energy Transport: Relaxation-Assisted 2DIR Measurements and Theoretical Studies. *J. Phys. Chem. B* **2011**, *115*, 11063−11073.
(63) Kasyanenko, V. M.; Lin, Z.; Rubtsov, G. I.; Donahue, J. P.; Rubtsov, I. V. Energy Transport via Coordination Bonds. *J. Chem. Phys.* **2009**, *131*, 154508.
(64) Lian, T.; Locke, B.; Kholodenko, Y.; Hochstrasser, R. M. Energy Flow from Solute to Solvent Probed by Femtosecond IR Spectroscopy: Malachite Green and Heme Protein Solutions. *J. Phys. Chem.* **1994**, *98*, 11648−11656.
(65) Tokmakoff, A.; Sauter, B.; Fayer, M. D. Temperature-Dependent Vibrational Relaxation in Polyatomic Liquids: Picosecond Infrared Pump−Probe Experiments. *J. Chem. Phys.* **1994**, *100*, 9035.
(66) Schweizer, K. S.; Chandler, D. Vibrational Dephasing and Frequency Shifts of Polyatomic Molecules in Solution. *J. Chem. Phys.* **1982**, *76*, 2296−2314.
(67) Eaves, J. D.; Tokmakoff, A.; Geissler, P. L. Electric Field Fluctuations Drive Vibrational Dephasing in Water. *J. Phys. Chem. A* **2005**, *109*, 9424−9436.
(68) Nee, M. J.; Baiz, C. R.; Anna, J. M.; McCanne, R.; Kubarych, K. J. Multilevel Vibrational Coherence Transfer and Wavepacket Dynamics Probed with Multidimensional IR Spectroscopy. *J. Chem. Phys.* **2008**, *129*, 084503.
(69) Khalil, M.; Demirdöven, N.; Tokmakoff, A. Coherent 2D IR Spectroscopy: Molecular Structure and Dynamics in Solution. *J. Phys. Chem. A* **2003**, *107*, 5258−5279.
(70) Ishikawa, H.; Kwak, K.; Chung, J. K.; Kim, S.; Fayer, M. D. Direct Observation of Fast Protein Conformational Switching. *Proc. Natl. Acad. Sci. U.S.A.* **2008**, *105*, 8619−8624.
(71) Morita, A.; Kato, S. Vibrational Relaxation of Azide Ion in Water: The Role of Intramolecular Charge Fluctuation and Solvent-Induced Vibrational Coupling. *J. Chem. Phys.* **1998**, *109*, 5511.
(72) Blanco-Rodriguez, A. M.; Ronayne, K. L.; Zalis, S.; Sykora, J.; Hof, M.; Vlcek, A. Solvation-Driven Excited-State Dynamics of $[Re(4\text{-}Et\text{-}Pyridine)(CO)_3(2,2'\text{-}Bipyridine)]^+$ in Imidazolium Ionic Liquids. A Time-Resolved Infrared and Phosphorescence Study. *J. Phys. Chem. A* **2008**, *112*, 3506−3514.
(73) Park, K.-H.; Jeon, J.; Park, Y.; Lee, S.; Kwon, H.-J.; Joo, C.; Park, S.; Han, H.; Cho, M. Infrared Probes Based on Nitrile-Derivatized Prolines: Thermal Insulation Effect and Enhanced Dynamic Range. *J. Phys. Chem. Lett.* **2013**, *4*, 2105−2110.
(74) Kauffman, G. W.; Jurs, P. C. Prediction of Surface Tension, Viscosity, and Thermal Conductivity for Common Organic Solvents Using Quantitative Structure-Property Relationships. *J. Chem. Inf. Comput. Sci.* **2001**, *41*, 408−418.
(75) Horng, M. L.; Gardecki, J. A.; Papazyan, A.; Maroncelli, M. Subpicosecond Measurements of Polar Solvation Dynamics: Coumarin 153 Revisited. *J. Phys. Chem.* **1995**, *99*, 17311−17337.
(76) Frenking, G.; Fröhlich, N. The Nature of the Bonding in Transition-Metal Compounds. *Chem. Rev.* **2000**, *100*, 717−774.
(77) Hocking, R. K.; Hambley, T. W. Database Analysis of Transition Metal Carbonyl Bond Lengths: Insight into the Periodicity of Π Back-Bonding, Σ Donation, and the Factors Affecting the Electronic Structure of the TM-CO Moiety. *Organometallics* **2007**, *26*, 2815−2823.
(78) Hill, J. R.; Ziegler, C. J.; Suslick, K. S.; Dlott, D. D.; Rella, C. W.; Fayer, M. D. Tuning the Vibrational Relaxation of CO Bound to Heme and Metalloporphyrin Complexes. *J. Phys. Chem.* **1996**, *100*, 18023−18032.
(79) Dlott, D. D.; Fayer, M. D.; Hill, J. R.; Rella, C. W.; Suslick, K. S.; Ziegler, C. J. Vibrational Relaxation in Metalloporphyrin CO Complexes. *J. Am. Chem. Soc.* **1996**, *118*, 7853−7854.
(80) Hill, J. R.; Dlott, D. D.; Fayer, M. D.; Peterson, K. A.; Rella, C. W.; Rosenblatt, M. M.; Suslick, S.; Ziegler, C. J. Vibrational Relaxation of Carbon Monoxide in Model Heme Compounds. 6-Coordinate Metalloporphyrins (M = Fe, Ru, Os). *Chem. Phys. Lett.* **1995**, *244*, 218−233.
(81) Lupinetti, A. J.; Fau, S.; Frenking, G.; Strauss, S. H. Theoretical Analysis of the Bonding between CO and Positively Charged Atoms. *J. Phys. Chem. A* **1997**, *101*, 9551−9559.
(82) Goldman, A. S.; Krogh-jespersen, K. Why Do Cationic Carbon Monoxide Complexes Have High C−O Stretching Force Constants and Short C−O Bonds? Electrostatic Effects, Not σ-Bonding. *J. Am. Chem. Soc.* **1996**, *7863*, 12159−12166.
(83) Fielicke, A.; von Helden, G.; Meijer, G.; Pedersen, D. B.; Simard, B.; Rayner, D. M. Size and Charge Effects on the Binding of CO to Late Transition Metal Clusters. *J. Chem. Phys.* **2006**, *124*, 194305.
(84) Singh, U. C.; Kollman, P. A. An Approach to Computing Electrostatic Charges for Molecules. *J. Comput. Chem.* **1984**, *5*, 129−145.
(85) Besler, B. H.; Merz, K. M.; Kollman, P. A. Atomic Charges Derived from Semiempirical Methods. *J. Comput. Chem.* **1990**, *11*, 431−439.

(86) Stewart, A. I.; Clark, I. P.; Towrie, M.; Ibrahim, S. K.; Parker, A. W.; Pickett, C. J.; Hunt, N. T. Structure and Vibrational Dynamics of Model Compounds of the [FeFe]-Hydrogenase Enzyme System via Ultrafast Two-Dimensional Infrared Spectroscopy. *J. Phys. Chem. B* **2008**, *112*, 10023−10032.
(87) Greetham, G. M.; Clark, I. P.; Weidmann, D.; Ashfold, M. N. R.; Orr-Ewing, A. J.; Towrie, M. Waveguide-Enhanced 2D-IR Spectroscopy in the Gas Phase. *Opt. Lett.* **2013**, *38*, 3596−3599.